ANALYSIS OF EVTOL MULTICOPTER WEIGHT AND POWER BUDGET AS A FUNCTION OF THE NUMBER OF ROTORS

Dmitrij Usov, dmitrij.usov@manchester.ac.uk, University of Manchester (United Kingdom)
Antonio Filippone, A.Filippone@manchester.ac.uk, University of Manchester (United Kingdom)
Nicholas Bojdo, nicholas.bojdo@manchester.ac.uk, University of Manchester (United Kingdom)

Abstract
In this work, we focused on predicting the power budget and weight variation of an electric, wingless multicopter operating in a typical UAM mission as a function of the total number of rotors in the propulsion group. The aerodynamic performance was obtained using the *actuator disk* inflow model, and weights were estimated based on semi-empirical scaling laws of the electrical components in the power train. The key aspect of this analysis procedure is that it accounted for the potential failure events that reflected on the power budget and weight of the rotorcraft. Results describe the weights of the propulsion system components, power requirements, and energy budget of the rotorcraft as a function of the total number of rotors. The main conclusion is that a larger number of rotors is beneficial for the rotorcraft's weight and power budget, for a number of rotors within the practical range, i.e. $N_P \in [6, 20]$. A global minimum exists for both energy budget requirements and MTOW if the efficiency of the power train degrades with an increasing number of rotors. Optimising multicopter for minimum weight can be misleading as it does not result in the most efficient configuration energy budget-wise.

1. INTRODUCTION

1.1. Problem Formulation

A considerable number of engineering problems need to be solved before eVTOL can become a realistic class of air vehicles [1]. One of those issues is that these new vehicle systems are very different from existing rotorcraft, there is very limited knowledge accumulated via design, manufacturing, flight testing, safety and operational costs. This paper addresses the power budget of an electrically powered VTOL and redundancy considerations aimed at defining an optimum number of rotors.

There is a wide range of conceptual eVTOL designs all over the world. According to the eVTOL database from the Vertical Flight Society (VFS) website [2], the multicopter population has nearly doubled between July 2020 and April 2021, as shown in Fig. 1.1. We summarised the population of electric multicopters and categorised it in terms of propulsion system design configuration. Most of these conceptual designs vary significantly from each other. For instance, the histogram in Fig. 1.2 represents a distribution of multicopter population based on propulsion system configuration in terms of a number of rotors. Despite the increase in the population size, the distribution of multicopter designs remained unchanged. Hence, there is no evidence that the conventional multicopter design exists or converges towards some conventional configuration.

Many proposed designs of eVTOL multicopter rely on distributed electric propulsion. Distributed Electric Propulsion (DEP) is a propulsion architecture that comprises a set of electrical motors-propeller arrangements placed around the aircraft that are mechanically independent of each other [3]. Therefore, the rotary-wing aircraft propulsion and control can be achieved using differential thrust through the quasi-instantaneous change in motor rotational speed. This reduces the mechanical complexity of the rotor systems [4], as the need for the intricate cyclic and collective control mechanism (swashplate) is eliminated while adding more freedom into configuration design [5].

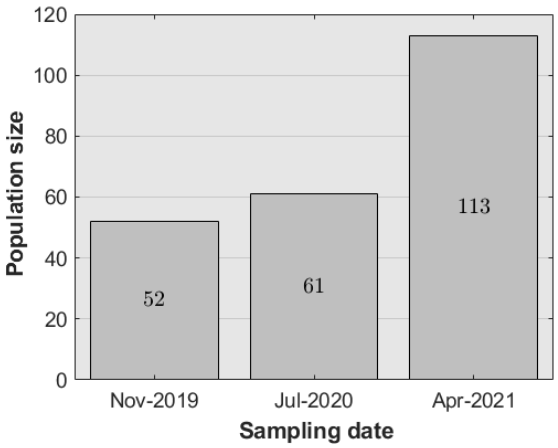

Figure 1.1: Mulicopter population growth.

Undoubtedly, the sizing and preliminary design methodology of small-scale electric multicopter UAVs has been addressed in previous literature. Unfortunately, recent studies on UAM aircraft mainly focused on aerodynamics and performance analysis but not on sizing and configuration design aspects of eVTOL multicopters. Barra et al. (2020) investigated the effects of the number of rotors on the power budget of an electric UAM multicopter [6]. However, the authors did not account for the redundancy and

Presented at 47th European Rotorcraft Forum, United Kingdom, 7-9th September, 2021

effect of the number of rotors on the aircraft's gross weight.

Because of the lack of technical knowledge and design tools, most conceptual eVTOL multicopters never go beyond the preliminary design stage. The motivation behind this work is to highlight the preliminary configuration design procedure and develop a sizing methodology suitable for the early-stage design of the eVTOL multicopter. This can be achieved by studying the relationship between the power budget and the number of rotors in the propulsion group. Therefore, clarifying considerations behind the choice of the propulsion group during the conceptual design stage.

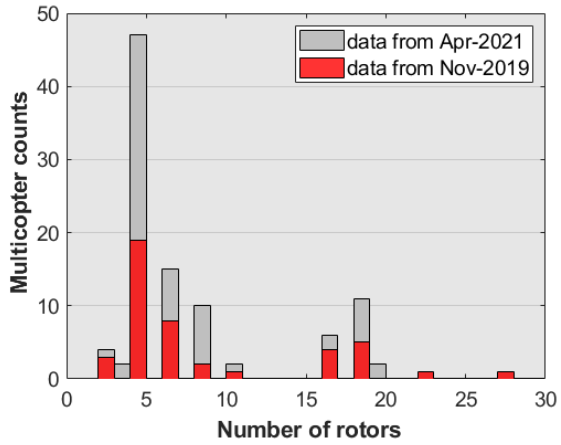

Figure 1.2: Number of rotors as the design choice for the multicopter configuration.

1.2. eVTOL Classification

The "eVTOL" is a generic term for any electrically driven aircraft that has the capability to take off and land vertically. There are five different types of eVTOL aircraft, shown in Fig. 1.3. Each eVTOL type has a distinctive design feature, mainly associated with the way how the aircraft produces lift and propulsive forces.

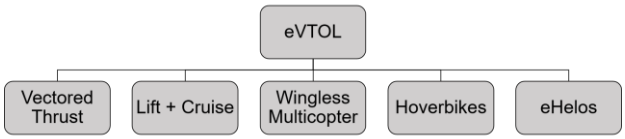

Figure 1.3: eVTOL classification.

For instance, ***Vectored Thrust*** employs tilting propulsors and uses any of them across the whole flight envelope. During axial flight regimes, the thrusters are tilted upwards to produce lift force. In forward flight regimes, such as cruise, the thrusters are in the horizontal position producing forward propulsive force, while the fixed wing generates the lift.

Lift + cruise are like vectored thrust eVTOLs, as both use a wing to generate thrust in forward flight. However, lift + cruise aircraft uses two independent sets of propulsors: "lifters" and "thrusters". Lifters are employed during the axial flight regime to produce vertical force, while thrusters are inoperative. Thrusters generate horizontal propulsive force during forward flight while lifters are off.

Wingless Multicopters is a type of Electric Vertical eVTOL aircraft that utilises any of its propulsors to produce both lift and thrust across all flight regimes. As the name suggests, this type of aircraft does not have a fixed wing. The wingless multicopter is considered as the best fit candidate for the Urban Air Mobility (UAM) intra-city (short-range) operations, where time in hover and axial flight regimes take a significant portion of the total flight time [7]. This is the case because electric multicopter has the largest actuation area compared to other eVTOL types.

Hoverbikes, also called ***Personal Flying Devices***, is a sub-group of wingless multicopters capable of transporting only one person (a pilot) who sits in a saddle or standing, similar to the biker.

Electric-helicopters or ***eHelos*** have a conventional single-rotor helicopter configuration where instead of a thermal engine, an electric motor is used. There is much scepticism around this approach. Moore et al. (2014) elaborated that new propulsion technologies do not integrate with conventional aircraft designs [5]. The first mass-produced helicopters were deployed in the 1940s. Since then, all design iterations and technological advancements to improve performance were made, accounting for the benefits and limitations of thermal engines. Therefore, simply substituting a thermal engine with an electric one might be misleading.

2. METHODOLOGY

As we aim to investigate the effects of propulsion system configuration on the gross weight, power, and energy budget of an arbitrary multicopter, we need to fix hyperparameters, such as net actuation area, reference tip speed, rotor solidity, induced power correction factor etc., to ensure that results are comparable. Therefore, the following assumptions were made at the beginning of the analysis:

1. The payload and a mission profile are fixed for the whole range of multicopters considered in the analysis.

2. Any given propulsion group consists of identical electronic speed controllers (ESCs), motors, and rotors.

3. Thrust is evenly distributed across all operating rotors in a given propulsion group.

4. All rotors are fixed-pitch, fixed-tilt, and variable-RPM.

5. The total actuation area is constant across all multicopters.

6. The actuation area of each rotor is constant within a given multicopter configuration.

For instance, a hexacopter's net actuation area equals a net actuation area of an octocopter.

$$\sum A_n|_{N_P=6} = \sum A_n|_{N_P=8} \quad (1)$$

2.1. Power Train Decomposition

The literature suggests that a power train of any electrical aircraft has an identical structure [8][9][10], which can be modelled by decomposing the power train into three main components: 1. Power generation device (PGD); 2. Power transfer device (PTD); 3. Power output device (POD). Fig. 2.1 shows a power train for generic electric aircraft.

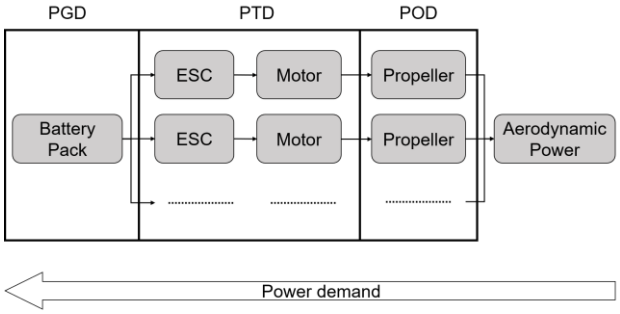

Figure 2.1: Power train representation of a generic electric aircraft with multiple propulsors

The electrical energy is stored in the battery pack and transferred through the power train to propellers, which convert shaft power to thrust. As electrical energy transits through sub-components in the power path, some fraction of the energy is dissipated due to non-ideal effects, such as internal resistance. The energy losses can be accounted for by assigning an electrical efficiency to each component in the power train as follows

$$P_n = \eta_{net} P_1 \quad (2)$$

and

$$\eta_{net} = \prod_{i=1}^{n} \eta_i \quad (3)$$

Where P_1 is the first power input starting from the energy source, P_n is the destination power in a power path of n components and η_{net} is the net power path efficiency.

However, efficiencies depend on many parameters and time. A sophisticated electrical model of each component is required to accurately predict dynamic efficiencies, which is out of this project's scope. Therefore, an assumption of steady-state efficiency of the ESC and the motor will be used in the analysis.

To estimate the weight of the propulsion system, first, it is required to calculate power requirements for each component. Each consecutive electrical component imposes a power requirement to the previous electrical component along the power path. Therefore, the power path must be analysed in reverse order, starting from aerodynamic power estimation.

A range of different propulsion systems up to 20 propellers is considered to capture aircraft weight and power budget variation as a function of propulsion group size. Only single open rotors are considered for the analysis, i.e., coaxial and ducted propeller configurations are neglected.

2.2. Redundancy Considerations

UAM multicopters will operate in densely populated and confined urban environments [11]. Consequently, the failure analysis considerations must be incorporated in the preliminary multicopter configuration design. Basset et al. (2018) have addressed failure considerations for UAM eVTOL aircraft [12]. The methodology and tools presented in the paper allow calculating optimal thrust re-distribution in case of a single and double motor failure event. The optimisation tool, called "Linf", aims to re-distribute thrust around the propellers to minimise required power while satisfying trim conditions. In the event of a single motor failure in a multicopter's propulsion system, the "Linf" solution cancels an opposite motor (relative to the failed motor) and increases thrust on the remaining operating motors [12].

We need to ensure that the aircraft can be trimmed after the occurrence of a single failure event. There are six equations on motions. Hence, we need at least the same amount of independent control variables to solve them. In a multicopter system, each individual rotor (variable-RPM only) counts as such control variable, plus roll and pitch control. Hence, the minimum number of operating rotors to fully satisfy the trim condition must be four. That introduces a lower limit on the operating number of rotors in the propulsion system of an arbitrary multicopter. To accommodate the single motor failure event, utilising the "Linf" failure management scheme, the lower bound of rotors in a multicopter's propulsion system must be six, which is also reported in [13]. In addition, cancelling the opposite motor implies that each rotor must have a geometrically opposite twin with an opposite sense of rotation (to satisfy torque balance), which means that the total number of rotors must be even.

A single event failure can be modelled as a loss of two rotors in the propulsion system. Effectively that reduces the net actuation area by two single rotor areas in a given propulsion system e.g.

$$A^* = (N_P - 2)A_n, \quad \text{for} \quad N_P \geq 6 \tag{4}$$

Where A^* is the effective actuation area after the occurrence of a motor failure event, N_P and A_n, is the total number of rotors and individual rotor area in a given propulsion group, respectively. For ease of use, we will be notating the number of operating motors in a given propulsion system as N_P^*, e.g.,

$$N_P^* = N_P, \quad \text{for } \textit{all motors operative} \tag{5}$$

$$N_P^* = N_P - 2, \quad \text{for } \textit{the single failure event} \tag{6}$$

As the gross operating weight is not affected by a rotor failure event (during the flight), the remaining rotors must provide sufficient lift to maintain aircraft airborne. That leads to an increase in induced velocity and, hence, induced power of each rotor. Therefore, motors must be overpowered to accommodate aircraft weight in case of a single failure event. The increase in maximum motor power would result in a greater propulsion system weight leading to higher thrust requirements, which would impose an even higher power demand on the motors. Hence, the solution to this problem requires an iterative process.

These effects are more apparent for propulsion systems with a relatively small number of rotors, as each rotor has a more significant contribution to the net actuation area and thrust generation. Fig. 2.2 shows the effect of redundancy consideration on the maximum power requirements for an 18-rotor configuration operating over a typical mission profile.

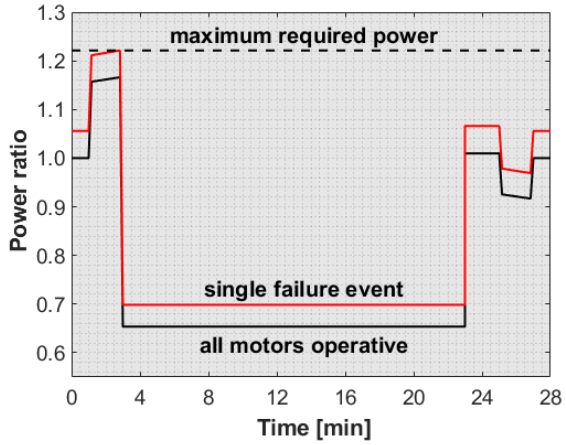

Figure 2.2: Power ratio profile over a typical UAM mission for 18-rotor multicopter configuration including and excluding redundancy considerations.

2.3. Aerodynamic Model

The aerodynamic performance of the rotors was estimated by means of momentum theory. Any technical data regarding conceptual UAM multicopters is not available in open access. Therefore, the choice of the low fidelity model was driven by the fact that it treats the rotor as a thin actuator disk where blades' geometry is not required. The main implication of the momentum theory is that it cannot capture any aerodynamic interactions between the rotors. However, the momentum theory is still well suited for this work as we are studying high-level trends between propulsion system size and the power budget.

The aerodynamic model was implemented in the MATLAB framework and validated against the UH-60A helicopter's experimental data [14]. The validation case is represented in Fig. 2.3, and it shows a good agreement between experimental and analytical results for the advance ratios greater than 0.1.

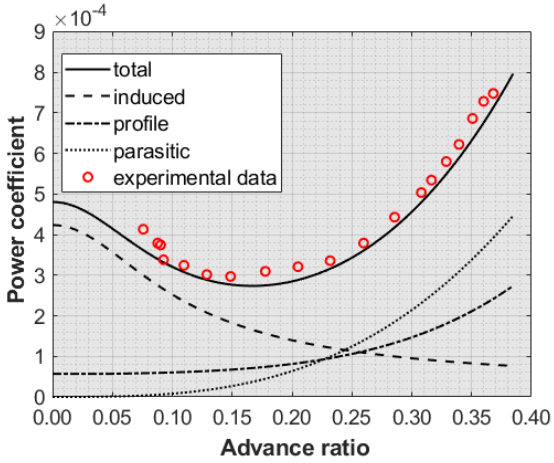

Figure 2.3: UH-60A main rotor power as a function of advance ratio at a blade loading of 0.8.

It is common to conduct the aerodynamic analysis in a non-dimensional format, which requires normalisation of performance parameters with respect to some fixed blade's tip speed. As discussed previously, eVTOL rotorcraft use DEP, which implies the use of fixed-pitch, variable-RPM rotors (in most cases). As tip speed becomes a control variable, performance parameters cannot be normalised while retaining the same physical meaning as in the nomenclature of classical helicopter (fixed-RPM, variable-pitch) analysis. Therefore, the analysis of variable-speed rotors must be accomplished in dimensional form.

2.3.1 Aerodynamic analysis procedure

As an entry point to the analysis, we need to evaluate the total thrust requirement of the whole multicopter system at a given operating point, e.g.

$$T = \sqrt{D^2 \cos^2(\gamma) + (D sin(\gamma) + W)^2} \quad (7)$$

Where W is the gross weight of an aircraft, γ is the flight path angle, and D is the net drag of an aircraft

$$D = \frac{1}{2}\rho V_\infty^2 f \quad (8)$$

Where ρ is the air density, V_∞ is the airspeed, and f is the equivalent flat plate area. Assuming that the thrust is evenly distributed across all running rotors in the propulsion system, the individual rotor thrust is

$$T_n = \frac{T}{N_P^*} \quad (9)$$

Hence, the induced velocity, v_i, at each rotor can be calculated by solving the equation below

$$T_n = 2\rho A_n v_i \sqrt{V_x^2 + (V_z + v_i)^2} \quad (10)$$

Where V_x and V_z are tangential and normal velocities relative to the rotor disk plane, which are given by

$$V_x = V_\infty \cos(\alpha), \qquad V_z = V_\infty \sin(\alpha) \quad (11)$$

Where α is the relative inflow angle, which can be written as

$$\alpha = \frac{\pi}{2} - \arctan\left(\frac{D\,sin(\gamma)+W}{D\,cos(\gamma)}\right) + \gamma \quad (12)$$

The total power P, for the whole multirotor system, can be described as the sum of the net induced power P_i, parasite power P_p, climb power P_c, and net profile power P_0. For instance,

$$P = P_i + P_p + P_c + P_0 \quad (13)$$

$$P = \kappa T v_i + D V_\infty + W V_c + P_0 \quad (14)$$

Where κ is the induced power correction factor and V_c is the climb velocity.

$$P_0 = \frac{N_b c \rho R_n}{8 V_{tip}}\left(V_{tip}^4 + 4\left(V_x V_{tip}\right)^2 + \frac{5}{8}V_x^4\right) C_{d0} N_P^* \quad (15)$$

Where N_b is the number of blades, c is the mean blade's chord, R_n is the rotor radius, V_{tip} is the blade's tip speed due to angular velocity, and C_{d0} is the blade's mean profile drag coefficient.

For multicopter configurations with a larger number of rotors, each individual rotor radius diminishes. Leading to a decrease in operating Reynolds number, hence, an increase in viscous losses. To account for these effects, we need to apply the Reynolds number correction factor, as follows

$$C_{d0} = C_{d0,ref}\left(\frac{Re}{Re_{ref}}\right)^{-n} \quad (16)$$

Where $C_{d0,ref}$ is the reference profile drag coefficient obtained at some reference Reynolds number Re_{ref}, Re is the operating Reynolds numbers, and n is the exponent.

From Eq. 15, the profile power, P_0, is proportional to the cube of the blade's tip speed. The increase in thrust can only be achieved through the differential RPM for fixed-pitch rotor blades. Unfortunately, momentum theory does not capture the dependency between rotor RPM and thrust. To overcome this limitation, we can be assumed that the rotor's thrust coefficient remains unchanged with the change in rotor tip speed. This property is documented in previous literature. For instance, the experimental work on small-scale UAV variable-RPM rotors at low Reynolds numbers suggests that the thrust coefficient is nominally dependent on the rotor speed [15][16]. Strictly speaking, an increase in RPM results in a proportional increase in thrust, while the thrust coefficient remains unchanged.

Furthermore, we cross-checked this behaviour with Peters-He Generalised Wake Model. Fig. 2.4 shows the tip speed effects on the rotor thrust coefficient. The plot was obtained for an XV-15 isolated rotor in hover. The thrust coefficient is weakly dependent on rotor tip speed, especially at low collective settings and tip Mach numbers.

Therefore, the rotor's tip speed after a single failure event can be estimated as

$$V_{tip}^* = V_{tip}\sqrt{\frac{N_P}{N_P^*}} \quad (17)$$

It can be noticed that the maximum increase in a rotor's tip speed appears when the N_P reaches the lower limit e.g.

$$V_{tip}^* = 1.2247 V_{tip}, \quad \text{at} \quad N_P = 6. \quad (18)$$

Due to a relatively small rotor radius, a typical operating range of multicopter's rotor tip speeds lies between Mach numbers 0.4 and 0.5 [17][18]. Thus, this assumption must be valid.

Once total power requirements are evaluated, we can find the power requirements of each rotor, which can be interpreted as

$$P_{shaft} = \frac{P}{N_P^*} \quad (19)$$

Where P_{shaft} is the motor's shaft power output, which equals to the rotor's aerodynamic power requirement.

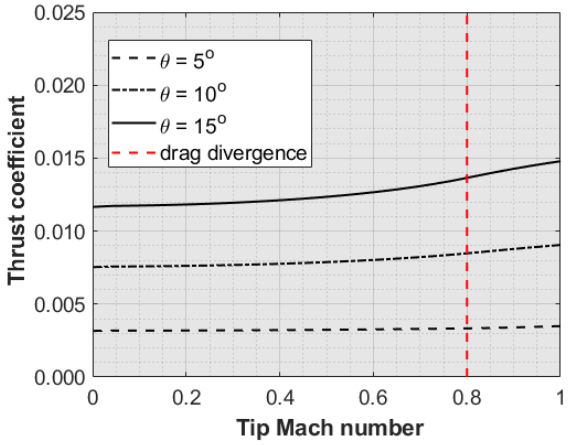

Figure 2.4: Thrust coefficient of XV-15 isolated rotor in hover as a function of rotor's angular velocity, at different collective pitch settings.

2.4. Weight Estimation

Propulsion system mass can be evaluated utilising empirical scaling laws for every sub-component in the power train. Generally, scaling laws are statistically derived from the small-scale UAV electrical hardware databases. The main concern is that UAM multicopters are typically two orders of magnitude heavier than their small-scale counterpart. This implies that the hardware database is not necessarily suitable for UAM like multicopters. That imposes uncertainty as some regression models must be extrapolated outside their database range.

Note that the selection of scaling laws in this paper carries a demonstrative purpose to describe the multicopter's preliminary sizing methodology. Scaling laws and efficiency maps are inputs to the analysis procedure. The selection of these regression models must be accomplished based on specific requirements and hardware that is available to a manufacturer.

Nevertheless, we decided to utilise the most conservative scaling laws (largest weight output for the same input parameter) that were found in the literature to demonstrate global trends between the number of rotors and power budget/weight of a multicopter.

2.4.1 Rotor group analysis

As discussed earlier, the rotor group is modelled as a set of identical propellers. The net equivalent disk area is consistent across a range of multicopter configurations and equals to a reference area i.e.

$$\sum_{n=1}^{N_P} A_n = N_P A_n = A \tag{20}$$

Hence, individual rotor radius can be expressed as

$$R_n = \sqrt{\frac{A}{\pi N_P}} = \frac{R}{\sqrt{N_P}} \tag{21}$$

Where R is the reference rotor radius in (m).

The most conservative propeller scaling approach is found to be Ampatis' model [8], and it is represented by the equation below.

$$W_r = 19.1432 R_n^{2.574} \tag{22}$$

Where W_r is the individual rotor weight in (N). The authors provided the coefficient of determination R^2, which equals to 0.98. Unfortunately, the sample size of this scaling law was not given. However, the authors have mentioned that they were interested in propellers with diameters between 0.08 and 0.5 meters [8].

2.4.2 Motor and ESC group analysis

The power requirement derived from the aerodynamic model can be interpreted as the electrical-motor maximum shaft power output. Hence, motor mass can be estimated directly after obtaining aerodynamic performance requirements. Johnson's model [19] was chosen for motor mass estimation as the most conservative approach found in the literature. Furthermore, it accounts for the accessories weight, such as ESC, inverter, and thermal management system. The scaling equations can be written as

$$W_m = 1.8691 Q_{max}^{0.8129} \tag{23}$$

Where W_m is an individual motor weight in (N), and Q_{max} is the maximum motor's torque (Nm). The maximum torque can be obtained from the maximum power requirements (Fig. 2.2) and operational RPM. According to [19], this regression equation was based on a sample of 64 motors, ranging from 20 to 550 hp and 100-10,000 RPM. The coefficient of determination is not provided. Instead, an average error is given to be 25%.

A conservative assumption of steady-state electronic ESC efficiency of 80% [20] across a whole range of propulsion groups is utilised in the analysis. The electric motors efficiency variation can notably affect the power budget estimates. Therefore, electric-motor efficiencies are modelled based on the statistical data found in the literature [21]. Fig. 2.5 depicts the experimental data and statistical regression model of electric-motor efficiency as a motor's nominal power function. The regression model can be written as

$$\eta_m = 0.0311 \ln(P_{max}) + 0.5776 \tag{24}$$

Where η_m is the motor efficiency and P_{max} is the motor's maximum rated power in (W). Typically, electric motors reach maximum efficiency at 30-50%

of the full load [21]. Thus, a single efficiency value obtained from Eq. 24 is used throughout the whole mission profile for a given propulsion system configuration.

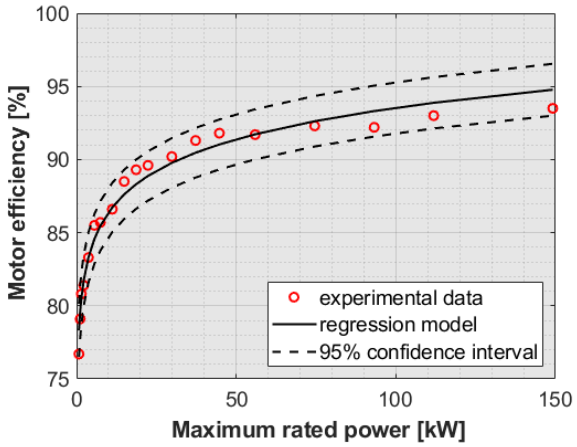

Figure 2.5: Experimental data and regression model of electric-motor efficiency as a function of maximum rated power.

2.4.3 Battery analysis

We utilised Gatti and Giulietti (2013) regression model to estimate the battery's weight as it outputs the largest battery mass estimate for the same energy capacity.

(25) $$E_b = 138.17 m_b - 0.0422$$

The equation above describes the relationship between the energy capacity, E_b in (Wh), and the battery mass, m_b in (kg). The first coefficient represents the gravimetric energy density, which lies at the lower boundary of the current battery technology level [19]. The battery set was comprised of 163 lithium-polymer (Li-Po) batteries from 7 different manufactures. The battery weight in the data set ranged from 0 to 1 kg. A coefficient of determination was not provided in the paper [22].

The battery power output requirements can be described as the aerodynamic power requirements accounting for the non-ideal losses in the motor and ESC.

(26) $$P_b = (\eta_{ESC}\eta_m)^{-1} P$$

Where P_b is the battery power output, η_{ESC} is the ESC's efficiency and η_m is the motor's efficiency.

The battery energy capacity can be obtained by integrating the mission profile power under normal operating conditions (see Fig. 2.2, all motors operative).

(27) $$E_b = (\eta_{net})^{-1} \int_{t_0}^{t_n} P(t)dt = \int_{t_0}^{t_n} P_b(t)dt$$

Where η_{net} is the net power path (battery to rotor) efficiency and, $P(t)$ is the aerodynamic power as a function of time, t_0 and t_n are the times at the start and the end of the mission, respectively.

2.4.4 Aircraft's Gross Weight Analysis

The gross aircraft weight can be estimated by adding weights of each sub-system in the power train, structural weight, and payload weight.

(28) $$W = (W_r + W_m)N_P + W_b + W_s + W_{pay}$$

(29) $$W_b = m_b g$$

(30) $$W_s = \frac{f_w}{1-f_w}\left((W_r + W_m)N_P + W_b + W_{pay}\right)$$

Where W_b is the battery weight, g is the gravitational acceleration, W_s is the structural weight, W_{pay} is the payload weight, and f_w is the structural weight fraction of the gross weight. All parameters are given in SI base units.

Once the aircraft's gross weight is estimated, we need to update thrust requirements and repeat the weight estimation procedure till the weight convergence criterion is achieved.

2.5. Mission Profile

According to the literature [6][11], a typical UAM intra-city mission consists of 6 stages: 1. Take-off; 2. Climb; 3. Cruise; 4. Hover; 5. Descent; 6. Landing. The mission profile was adopted from Barra et al. (2020), summarised in Table 1.

Mission Stage	*Duration [min]*	*Vertical speed [m/s]*	*Horizontal speed [m/s]*	*Altitude [m]*
Take-off	1	0	0	0
Climb	2	3	0	300
Cruise	20	0	20	300
Hover	2	0	0	300
Descent	2	-3	0	0
Landing	1	0	0	0

Table 1: Mission profile.

2.6. Aircraft Specifications

Most conceptual designs in [2] specify their maximum passenger capacity as between 1 and 2 people. Unfortunately, whether this number includes pilot or not is inconsistent throughout the population data. Thus, we assumed maximum passenger capacity as 2, including pilot and the payload was set to be 200 kg. The structural weight incorporates arms, airframe, and landing gear. The structural weight fraction was set to 30% of the maximum take-off weight (MTOW) [23] and assumed to be fixed for

the whole range of multicopters examined in this work. Please note, for electric aircraft, the MTOW is the sum of operating empty weight and maximum payload weight.

Specific parameters that we used in the analysis are summarised in Table 2.

Parameter	*Notation*	*Value*	*Unit*
Net actuation area	A	74.79	m^2
Blade reference profile drag coefficient	$C_{d0,ref}$	0.010	-
Equivalent flat plate area	f	2.32	m^2
Structural weight fraction	f_w	0.30	-
Reference tip Mach number (all motors operative)	M_{tip}	0.40	-
Number of blades	N_b	2	-
Reynolds number correction factor exponent	n	0.40	-
Reference Reynold number	Re_{ref}	1e6	-
Payload weight	W_{pay}	1,962	N
ESC efficiency	η_{ESC}	0.80	-
Induced power correction factor	κ	1.150	-
Rotor solidity	σ	0.065	-

Table 2: Rotorcraft hyperparameters.

3. RESULTS

Fig. 3.1 illustrates the maximum rated power to hover power ratio as a function of the number of rotors. The figure shows that the maximum power ratio occurs at six rotors and then gradually declines as the number of rotors increases. As discussed previously, the propulsion system requires at least six rotors to safely accommodate a single failure event. Otherwise, it would be impossible to trim the multicopter if the motor fails. For a given payload and fixed mission profile, the power ratio of a hexacopter configuration is approximately 13.4% higher compared to a 20-rotor configuration.

The same trend is observed for the gross and sub-systems weight of the aircraft. Fig. 3.2 shows a range of normalised weight ratios with respect to the baseline configuration (20-rotors). The results show that all weights are diminishing with an increase in propulsion group size. The MTOW of a hexacopter configuration is 19.2% higher than the 20-rotor configuration. As was expected, the MTOW and battery weight ratios are in agreement. This is the case because the battery is the heaviest sub-component of the electric aircraft [10]. The motor group is the most sensitive sub-system to the change in the number of rotors, as motors must be significantly overpowered for configurations with fewer rotors.

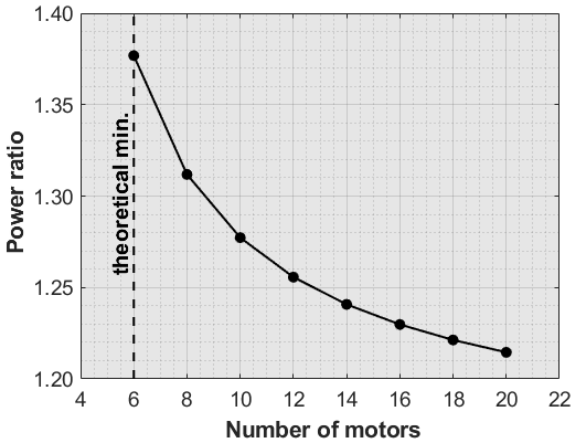

Figure 3.1: Maximum rated power to hover power ratio for a range of multicopter propulsion system configurations.

Fig. 3.3 shows the energy budget for a range of multicopter configurations at a given mission and fix payload. The energy requirements were normalised to the 20-rotor configuration. From the figure, it can be noted that the minimum energy requirement occurs at a 12-rotor configuration. This is the case because of the motor efficiency effect. Smaller motors are less efficient compared to their larger counterpart [21], as mentioned previously. Therefore, that imposes a higher energy requirement on the battery, leading to higher battery weight. However, the weight of all other sub-systems reduces with an increase in the number of rotors in the propulsion system (subject to employed scaling laws). Thus, the overall weight of an aircraft diminishes. However, this is only true for the $N_P \in [6, 20]$. If we hypothetically extend number of rotors to some large arbitrary number, that would allow us to see the global trends more evidently.

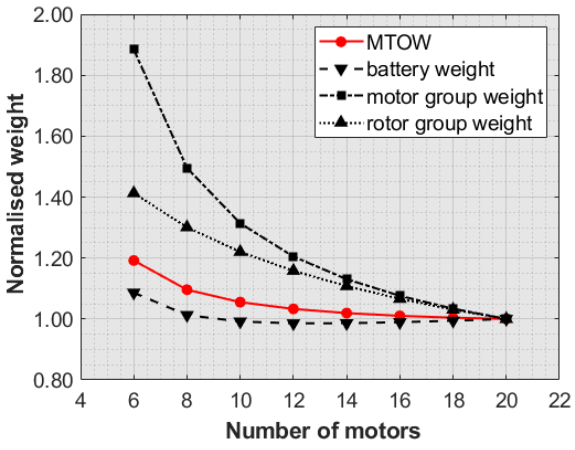

Figure 3.2: Normalised weight as a function of the number of rotors relative to the 20-rotor configuration.

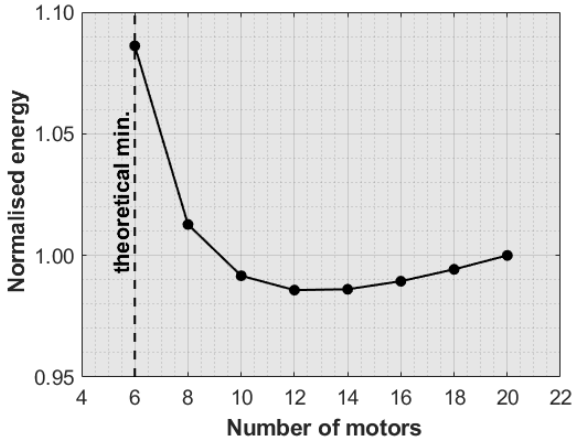

Figure 3.3: Energy requirements as a function of a number of rotors, normalised to 20-rotor configuration.

Fig. 3.4 depicts normalised MTOW and energy budget requirements for an extended range of propulsion systems. Now, we can see that a global minimum exists both for aircraft's maximum weight and energy requirement at 32-rotor and 12-rotor configuration, respectively. However, the most striking result that emerges from the data is that minimum energy budget requirements lag the minimum MTOW of the multicopter. This essentially means that weight optimal multicopter configuration is not the most efficient energy-wise.

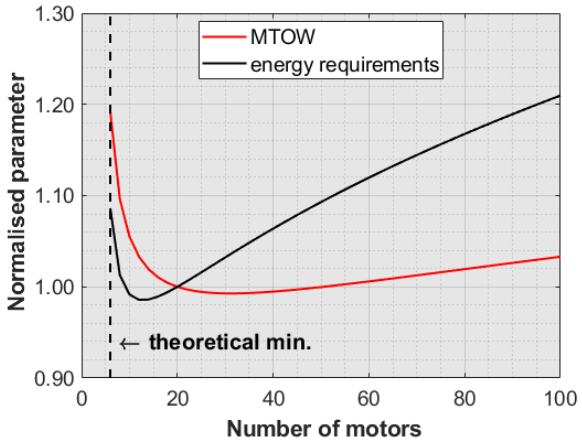

Figure 3.4: Global trends of MTOW and energy budget requirements for an extended range of propulsion systems, normalise to 20-rotor configuration.

4. CONCLUSION

We have presented the methodology for estimating electric multicopter's weight and power budget based on the number of rotors in the propulsion system while accounting for the potential failure events in the power train. A significant source of uncertainty in this method is the use of scaling laws that were derived from the small-scale UAV hardware databases due to the scarcity of technical data regarding electric components for UAM-scale multicopters.

Nevertheless, based on regression models (which we believe are the most conservative), a mission profile and failure event management approach employed in the analysis, the results of this study indicate that:

- Increasing the number of rotors in the propulsion system drives down power budget requirements and the maximum weight of a multicopter for a fixed mission profile and payload, for a practical range of rotors, $N_P \in [6, 20]$.
- The energy budget and MTOW have a global minimum if the efficiency of the power train degrades with an increase in the propulsion group size.
- Minimum MTOW configuration does not necessarily coexist with minimum energy configuration.

To conclude, the methodology described in the paper shows analysis procedures and considerations needed for UAM multicopter preliminary analysis. The described methodology is not limited to regression models, hyperparameters and mission profile selected in this work.

5. ACKNOWLEDGEMENTS

This research is part-funded by the UK Research Councils (EPSRC) *Methods and Experiments for Rotorcraft* (Mentor), Grant EP/S010092/1, the UK Vertical Lift Network, EPSRC Grant EP/M018164/1, and a Presidential PhD Scholarship at the University of Manchester.

6. NOMENCLATURE

ABBREVIATIONS

DEP	*Distributed Electric Propulsion*
ESC	*Electronic Speed Controller*
eVTOL	*Electric Vertical Take-off and Landing*
Li-Po	*Lithium Polymer*
MTOW	*Maximum Take-off Weight*
PGD	*Power Generation Device*
POD	*Power Output Device*
PTD	*Power Transfer Device*
RPM	*Revolutions per Minute*
VFS	*Vertical Flight Society*
VTOL	*Vertical Take-off and Landing*
UAM	*Urban Air Mobility*
UAV	*Unmanned Arial Vehicle*

GREEK SYMBOLS

α	=	*Angle of Attack [rad]*
γ	=	*Flight Path Angle [rad]*
η_{ESC}	=	*ESC Efficiency [-]*
η_i	=	*Efficiency of i-th Component in the Power Train [-]*
η_m	=	*Electric Motor Efficiency [-]*
η_{net}	=	*Power Train Efficiency [-]*
κ	=	*Induced Power Correction Factor [-]*
ρ	=	*Atmospheric Density [kgm^{-3}]*
σ	=	*Rotor Solidity [-]*

ROMAN SYMBOLS

A	=	*Net Actuation Area/Reference Area [m^2]*
A_n	=	*Single Rotor Area in a Given Propulsion Group [m^2]*
A^*	=	*Effective Actuation Area [m^2]*
c	=	*Mean Chord of a Rotor in a Given Propulsion Group [m]*
C_{d0}	=	*Blade Profile Drag Coefficient [-]*
$C_{d0,ref}$	=	*Blade Reference Profile Drag Coefficient [-]*
D	=	*Aircraft's Net Drag [N]*
E_b	=	*Battery Energy Capacity [Wh]*
f	=	*Equivalent Flat Plate Area [m^2]*
f_w	=	*Structural Weight Fraction [-]*
g	=	*Gravitational Acceleration [ms^{-2}]*
N_b	=	*Number of Blades [-]*
N_P	=	*Total Number of Rotors in a Given Propulsion System [-]*
N_P^*	=	*Number of Operational Rotors in a Given Propulsion System [-]*
m_b	=	*Battery's Mass [kg]*
P	=	*Aerodynamic Power [W]*
P_0	=	*Net Profile Power [W]*
P_1	=	*Power Output of the 1-st Component in the Power Train [W]*
P_b	=	*Battery Power Output [W]*
P_c	=	*Climb Power [W]*
P_i	=	*Net Induced Power [W]*
P_i	=	*Power Output of the i-th Component in the Power Train [W]*
P_{max}	=	*Motor's Maximum Rated Power [W]*
P_n	=	*Power Output of the Last Component in the Power Train [W]*
P_p	=	*Parasitic Power [W]*
P_{shaft}	=	*Motor's Shaft Output Power [W]*
Q_{max}	=	*Motor's Maximum Torque Output [Nm]*
R	=	*Reference Rotor Radius [m]*
R_n	=	*Single Rotor Radius in a Given Propulsion Group [m]*
Re	=	*Reynolds Number [-]*
Re_{ref}	=	*Reference Reynolds Number [-]*
T	=	*Net Thrust [N]*
T_n	=	*Single Rotor Thrust in a Given Propulsion Group [N]*
V_c	=	*Vertical Speed [ms^{-1}]*
V_{tip}	=	*Reference Tip Speed [ms^{-1}]*
V_{tip}^*	=	*Adjusted Tip Speed After Single Motor Failure Event [ms^{-1}]*
V_x	=	*Tangential Velocity to the Rotor Disk [ms^{-1}]*
V_z	=	*Normal Velocity to the Rotor Disk [ms^{-1}]*
V_∞	=	*Airspeed [ms^{-1}]*
v_i	=	*Induced Velocity [ms^{-1}]*
W	=	*Aircraft's Gross Weight [N]*
W_b	=	*Battery's Weight [N]*
W_m	=	*Single Motor's Weight [N]*
W_{pay}	=	*Payload Weight [N]*
W_r	=	*Single Rotor Weight [N]*
W_s	=	*Structural Weight [N]*

7. REFERENCES

[1] A. Filippone and G. N. Barakos, "Rotorcraft systems for urban air mobility: A reality check," in *Aeronautical Journal*, Jan. 2021, vol. 125, no. 1283, pp. 3–21, doi: 10.1017/aer.2020.52.

[2] The Vertical Flight Society, "eVTOL Aircraft Directory," *Electric VTOL News, by the Vertical Flight Society*, 2021. https://evtol.news/aircraft (accessed Jul. 02, 2021).

[3] H. D. Kim, A. T. Perry, and P. J. Ansell, "A Review of Distributed Electric Propulsion Concepts for Air Vehicle Technology," in *2018 AIAA/IEEE Electric Aircraft Technologies Symposium, EATS 2018*, 2018, pp. 1–21, doi: 10.2514/6.2018-4998.

[4] Y. Tanabe *et al.*, "Numerical simulations of aerodynamic interactions between multiple rotors," in *42nd European Rotorcraft Forum 2016*, 2016, vol. 1, pp. 619–620.

[5] M. D. Moore and B. Fredericks, "Misconceptions of electric propulsion aircraft and their emergent aviation markets," *52nd Aerosp. Sci. Meet.*, pp. 1–17, 2014.

[6] F. Barra, M. Scanavino, and G. Guglieri, "A methodology for multirotor aircraft power budget analysis," *Aircr. Eng. Aerosp. Technol.*, vol. 92, no. 6, pp. 909–916, 2020, doi: 10.1108/AEAT-09-2019-0183.

[7] A. Bacchini and E. Cestino, “Electric VTOL configurations comparison,” *Aerospace*, vol. 6, no. 3, p. 26, Feb. 2019, doi: 10.3390/aerospace6030026.

[8] C. Ampatis and E. Papadopoulos, “Parametric Design and Optimization of Multi-Rotor Aerial Vehicles,” in *Springer Optimization and Its Applications*, vol. 91, 2014, pp. 1–25.

[9] T. Nam, D. S. Soban, and D. N. Mavris, “A generalized aircraft sizing method and application to electric aircraft,” *Collect. Tech. Pap. - 3rd Int. Energy Convers. Eng. Conf.*, vol. 1, no. August, pp. 598–615, 2005, doi: 10.2514/6.2005-5574.

[10] O. Gur and A. Rosen, “Optimizing electric propulsion systems for unmanned aerial vehicles,” *J. Aircr.*, vol. 46, no. 4, pp. 1340–1353, 2009, doi: 10.2514/1.41027.

[11] M. D. Patterson, K. R. Antcliff, and L. W. Kohlman, “A proposed approach to studying urban air mobility missions including an initial exploration of mission requirements,” in *Annual Forum Proceedings - AHS International*, 2018, vol. 2018-May.

[12] P. M. Basset, B. D. Vu, P. Beaumier, G. Reboul, and B. Ortun, “Models and methods at ONERA for the presizing of EVTOL hybrid aircraft including analysis of failure scenarios,” *Annu. Forum Proc. - AHS Int.*, vol. 2018-May, 2018.

[13] C. Silva, W. Johnson, K. R. Antcliff, and M. D. Patterson, “VTOL urban air mobility concept vehicles for technology development,” *2018 Aviat. Technol. Integr. Oper. Conf.*, pp. 1–16, 2018, doi: 10.2514/6.2018-3847.

[14] W. Johnson, “NDARC - NASA design and analysis of rotorcraft validation and demonstration,” 2010.

[15] G. K. Ananda, R. W. Deters, and M. S. Selig, “Propeller induced flow effects on wings at low Reynolds numbers,” 2013, doi: 10.2514/6.2013-3193.

[16] J. Brandt and M. Selig, “Propeller Performance Data at Low Reynolds Numbers,” 2011, doi: 10.2514/6.2011-1255.

[17] P. V. Diaz and S. Yoon, “Computational Study of the Side-by-Side Urban Air Taxi Concept,” in *AIAA Scitech 2020 Forum*, 2020, vol. 1 PartF, doi: 10.2514/6.2020-0302.

[18] P. V. Diaz and S. Yoon, “Computational study of nasa’s quadrotor urban air taxi concept,” in *AIAA Scitech 2020 Forum*, 2020, vol. 1 PartF, doi: 10.2514/6.2020-0302.

[19] W. Johnson, C. Silva, and E. Solis, “Concept vehicles for VTOL air taxi operations,” 2018.

[20] A. Gong and D. Verstraete, “Development of a dynamic propulsion model for electric UAVs,” in *APISAT 2015 - 7th Asia-Pacific International Symposium on Aerospace Technology*, 2015, pp. 206–217, Accessed: May 29, 2020. [Online]. Available: https://www.researchgate.net/publication/285581158_Development_of_a_dynamic_propulsion_model_for_electric_UAVs.

[21] C. M. Burt, X. Piao, F. Gaudi, B. Busch, and N. N. Taufik, “Electric motor efficiency under variable frequencies and loads,” *J. Irrig. Drain. Eng.*, vol. 134, no. 2, pp. 129–136, 2008, doi: 10.1061/(ASCE)0733-9437(2008)134:2(129).

[22] M. Gatti and F. Giulietti, “Preliminary design analysis methodology for electric multirotor,” in *IFAC Proceedings Volumes (IFAC-PapersOnline)*, Jan. 2013, vol. 2, no. PART 1, pp. 58–63, doi: 10.3182/20131120-3-FR-4045.00038.

[23] M. Budinger, A. Reysset, A. Ochotorena, and S. Delbecq, “Scaling laws and similarity models for the preliminary design of multirotor drones,” *Aerosp. Sci. Technol.*, vol. 98, p. 105658, Mar. 2020, doi: 10.1016/j.ast.2019.105658.